Dynamic Topography Change of the Eastern United States Since 3 Million Years Ago

David B. Rowley,[1]* Alessandro M. Forte,[2] Robert Moucha,[3] Jerry X. Mitrovica,[4] Nathan A. Simmons,[5] Stephen P. Grand[6]

Sedimentary rocks from Virginia through Florida record marine flooding during the mid-Pliocene. Several wave-cut scarps that at the time of deposition would have been horizontal are now draped over a warped surface with a maximum variation of 60 meters. We modeled dynamic topography by using mantle convection simulations that predict the amplitude and broad spatial distribution of this distortion. The results imply that dynamic topography and, to a lesser extent, glacial isostatic adjustment account for the current architecture of the coastal plain and proximal shelf. This confounds attempts to use regional stratigraphic relations as references for longer-term sea-level determinations. Inferences of Pliocene global sea-level heights or stability of Antarctic ice sheets therefore cannot be deciphered in the absence of an appropriate mantle dynamic reference frame.

The continental margin of the East Coast of the United States is the archetypal Atlantic-type or passive-type continental margin (*1*). Such margins have been thought to overlay a mantle that is entirely passive (*2*). As a consequence, passive-type margins are generally interpreted as having simple stratigraphic histories controlled by the interplay between thermally driven subsidence, sediment loading, compaction, and sea-level variations (*3*, *4*). Flexural responses of the lithosphere resulting from off-shore sediment loading (*5*, *6*) and, less frequently, onshore erosional unloading (*7*) are also recognized as potentially important (*4*–*6*). These assumptions underpin the rationale for the use of the U.S. East Coast margin in determining global long-term [≥ 0.1 million years (My)] sea-level variations (*4*–*6*, *8*, *9*).

The mantle is not a passive player. Mantle flow influences surface topography, through perturbations of the dynamic topography, in a manner that varies both spatially and temporally. As a result, it is difficult to invert for the global long-term sea-level signal and, in turn, the size of the Antarctic Ice Sheet by using East Coast shoreline data (*10*). Factors that need to be considered include flow associated with the negative buoyancy of the subducted Farallon slab (*10*–*14*) and the coupled shallower westward flow of hotter man-

[1]Department of the Geophysical Sciences, 5734 South Ellis Avenue, The University of Chicago, Chicago, IL 60637, USA. [2]GEOTOP—Université du Québec à Montréal CP 8888, succursale Centre-Ville Montréal, Québec H3C 3P8, Canada. [3]Department of Earth Sciences, 204 Heroy Geology Laboratory, Syracuse University, Syracuse, NY 13244, USA. [4]Department of Earth and Planetary Sciences, Harvard University, 20 Oxford Street, Cambridge, MA 02138, USA. [5]Atmospheric, Earth, and Energy Division, Lawrence Livermore National Laboratory, Livermore, CA 94551, USA. [6]Jackson School of Geological Sciences, University of Texas at Austin, Austin, TX 78712, USA.

*Corresponding author. E-mail: drowley@uchicago.edu

Downloaded from http://science.sciencemag.org/ on January 24, 2017

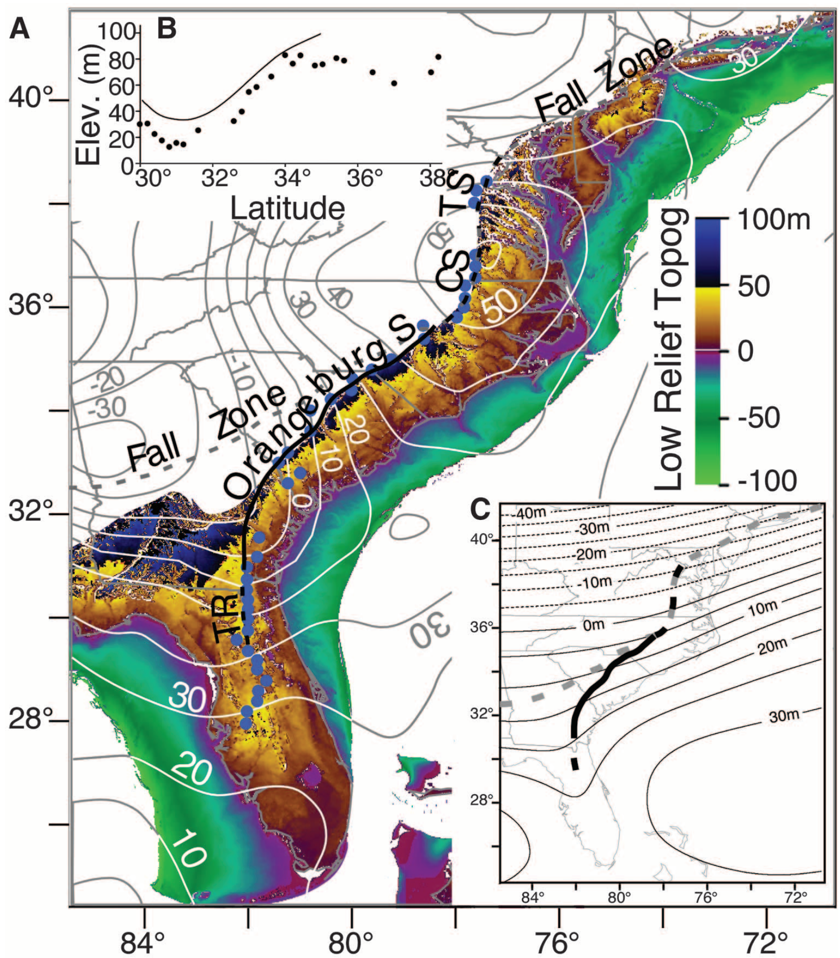

Fig. 1. Post–mid-Pliocene warping and incision of the Coastal Plain. (**A**) Present topography based on ETOPO1 emphasizing the incised, low-relief, mid-Pliocene flooding surface of the East Coast Coastal Plain, highlighting (black solid and dashed line) the locations of the Orangeburg, Chippenham (CS), Thornburg (TS) wave-cut scarps and Trail Ridge (TR) and (blue dots) sites with preserved mid-Pliocene (Yorktown, Duplin, Chorlton, and Cypresshead Formations) strata. Superimposed are contours showing an estimate of the amplitude of the post–3-Ma change in the dynamic topography based on TX2007 V2 model. The dynamic topography change is shown by the contours with a 10-m contour interval, white where they are superimposed on the topography. (**B**) Inset graph of the height of the Orangeburg Scarp as a function of latitude (solid line) based on (*26*) and the highest preserved mid-Pliocene marine sedimentary rocks as a function of latitude (dots). (**C**) Contours of GIA-induced relative sea level change based on the V2 viscosity profile (supplementary text) with a 5-m contour interval. The Orangeburg, Chippenham, and Thornburg Scarps are indicated by the thick black line; the Fall Zone is the thick dashed gray line.

tle (*10*, *12*, *15*). The latter produces, at least locally, changes in buoyancy and associated shorter wavelength changes in dynamic topography. Both factors confound local estimates of long-term sea-level variations (*15*).

The Coastal Plain is characterized by a sequence of marine and nonmarine sedimentary units that range from at least Early Cretaceous to present in age. These units generally thicken eastward to more than 12 km (*16*–*19*). This package unconformably overlies pre-Mesozoic crystalline rocks, as well as Triassic/Jurassic rift-basin strata, and pinches out to the west along the Fall Zone (Fig. 1A). Models of the depositional architecture of this margin have been developed on the basis of combinations of seismic stratigraphy and drilling (*9*, *18*, *19*) in order to better understand its evolution (*4*–*6*, *20*). These models have also been used to infer global sea-level history by solving for the contributions of thermal subsidence, sediment loading and compaction, flexural loading, and sediment delivery while assuming that the only remaining unknown is the contribution from changes in sea level. Most attempts have focused on the New Jersey segment of this margin (*4*–*6*, *9*, *21*). A local and temporally limited sea-level estimate has been made by using the mid-Pliocene Orangeburg Scarp as a marker (*8*). In this particular example, after correction for ~50 ± 18 m of post–mid-Pliocene uplift derived from a local estimate of stream incision rate (*22*), the Orangeburg Scarp has been inferred to have had an elevation of 35 ± 18 m, which has been taken to indicate the height of the mid-Pliocene sea level (*8*). This height would imply collapse of the Greenland and West Antarctic Ice Sheets and potentially considerable melting of the East Antarctic Ice Sheet during the mid-Pliocene climate optimum (*23*–*25*). However, the Pliocene strandline and immediately adjacent shallow marine sediments are not preserved at constant elevation along the Coastal Plain (Fig. 1B) (*26*). Thus, the Orangeburg Scarp is not a good reference for sea-level determinations for the Pliocene. Instead, we used the scarp as a marker for characterizing the processes that have warped the continental margin subsequent to 4 to 3 million years ago (*27*).

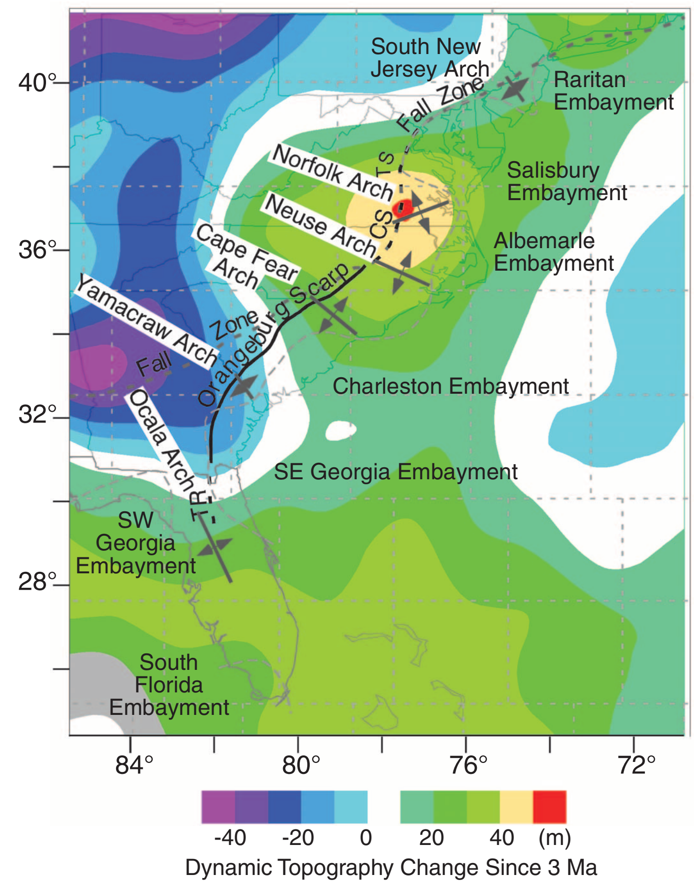

Fig. 2. Calculated dynamic topography change since 3 Ma. Locations of features associated with East Coast Coastal Plain geology after (*36*). The Fall Zone marks the approximate landward erosional edge of the Early Cretaceous to Cenozoic Coastal Plain strata. Color image is the distribution of retrodicted dynamic topography change based on TX 2007 V2 results. Dashed gray rectangular boxes outline the underlying resolution of the Simmons *et al*. (*33*, *34*) joint seismic-geodynamic tomography inversion. The Orangeburg and correlative scarps pass over the center of the maximum of retrodicted dynamic topography change since 3 Ma.

To assess the processes responsible for the post–mid-Pliocene warping of this margin, we developed a model of the Coastal Plain that accounts for mantle dynamics (*10*) and glacial isostatic adjustment (GIA) (*28*). Formation of karsts can also induce uplift (*29*). However, because carbonates are scarce north of Florida, we ignored this effect. Potential contributions from flexural warping because of offshore sediment loading and erosional unloading (*7*, *30*) were assessed (supplementary text) but were deemed too uncertain to yield reliable estimates for the current analysis. In addition, it is shown below that the majority of the warping can be accounted for by dynamic topography and GIA alone.

Our analysis focused on the variably incised, mid-Pliocene, low-relief flooding surface that characterizes the geomorphology of the eastern seaboard coastward of the Orangeburg and equivalent wave-cut scarps that define the landward edge of this surface (Fig. 1A). The Orangeburg and correlative scarps would have been horizontal at the time of formation; the adjacent mid-Pliocene shallow marine rocks and associated flooding surface would have been largely undissected and would have sloped gently eastward in a manner comparable to the modern shallow shelf. Therefore, the warping (Fig. 1B) and incision of this low-relief flooding surface primarily reflects post–mid-Pliocene relative uplift together with erosional down-cutting by rivers and streams that traverse the eastern Coastal Plain. A reasonable test of our modeling will be the retrodiction of this flooding surface to a configuration comparable to the modern shelf.

We calculated global mantle convective flow by following the approach of (*10*, *15*, *31*, *32*) with the tomography models TX2007 (*33*) and TX2008 (*34*), in which global seismic data together with a range of convection-related observables (present-day surface topography, free air gravity, plate velocities, and core-mantle boundary excess ellipticity) were jointly inverted to yield the three-dimensional (3D) distribution of density in the mantle (*34*) that is consistent with seismic, geodynamic, and mineral physics data. The underlying physical basis of this model is described in detail by Forte (*35*). We considered two different models of the radial distribution of viscosity, V1 and V2 (*10*, *31*, *32*), and these, together with the two different inversions (TX2007 and TX2008) for mantle density, provide four alternative models for predictions of time varying dynamic topography (see supplementary materials).

The 3D distribution of mantle buoyancy, when integrated with estimates of the radial distribution of viscosity, allows the computation of the instantaneous global flow field (*31*). With this in hand, we iteratively computed a global backward advection solution brought forward in time with a full convection calculation to estimate the vertical stresses acting on the base of the crust arising from flow in the mantle (*10*, *32*). These time-dependent vertical stresses generate a globally distributed dynamic topography that warps Earth's

Downloaded from http://science.sciencemag.org/ on January 24, 2017

surface. The difference between the present-day dynamic topography and estimates of past dynamic topography yields the change in dynamic topography as a function of time (Figs. 1 and 2 and fig. S1). The variations in height of the Orangeburg Scarp and related sediments (Fig. 1B) is well correlated, in latitude, with our estimates of the dynamic topography change since 3 million years ago (Ma). Both are high in Florida, decrease toward the north in the Southeast Georgia Embayment (~31°N), and then rise again farther north in the vicinity of the Cape Fear, Neuse, and Norfolk arches (Fig. 2).

The height of the Orangeburg Scarp rises more quickly starting north of 32°N than the estimates of dynamic topography change since 3 Ma (fig. S1). We attribute this misfit primarily to differences in the spatial scales of these data sets and to uncertainties in the tomography-based flow calculation. The joint seismic-geodynamic constrained tomography model has a minimum horizontal spatial resolution of 270 km by 270 km (*34*) (Fig. 2). It thus resolves mantle heterogeneity on a length scale substantially greater than the geological data being considered, whose variations are known to less than a kilometer resolution. In this regard, it is important to emphasize that our estimates of dynamic topography change are derived from full global mantle convection solutions and have not been adjusted or in any way tuned to yield better fits to the observed warping of the Orangeburg and correlative scarps.

Despite the longer-wavelength character of the seismic tomography constrained mantle flow calculations, there is a good spatial correlation between the maxima of the estimated changes in dynamic topography since 3 Ma and relative incision of the mid-Pliocene flooding surface (Fig. 1). Regions in Georgia with limited retrodicted changes in dynamic topography are characterized by limited fluvial incision into this surface. In contrast, farther north, where the retrodicted amplitude of dynamic topography change increases, the intensity of dissection increases concomitantly, and both reach a maximum in the vicinity of Chesapeake Bay (Figs. 1 and 2). The amount of incision of the low-relief flooding surface is about 50 ± 10 m in this region, in accord with the retrodicted amplitude of dynamic topography change since 3 Ma. This implies that a large fraction of the Coastal Plain geomorphology, at least shoreward of the Orangeburg Scarp, is a result of the interaction between flooding-related planation and subsequent dynamic topography induced uplift and fluvial incision within the last 3 My.

The principal outstanding feature of the dynamic topography retrodictions is the pattern of variable uplift along the East Coast of the United States (fig. S1). The origin of this uplift can be directly traced to the existence of hot, buoyant material in the shallow (<250 km) mantle under this region, with additional contributions resulting from the "far-field" advection of hot mantle rising from beneath Bermuda (figs. S2 and S3). The impact of this active, buoyant material on the upper-mantle convective flow field is shown in fig. S2, where one may note that the centers of upwelling mantle under the eastern margin of the United States are directly correlated with (and contributing to) the pattern of recent, post-Pliocene uplift of the coastal plain (fig. S3). We conclude that this aspect of the mantle flow field has played a large role in the topographic evolution of the eastern seaboard.

GIA refers to the deformational, gravitational, and rotational adjustment of Earth in consequence of the Late Pleistocene glacial cycles. The U.S. East Coast is mostly located on the peripheral bulge of the Laurentide ice complex, and it has been continuously subsiding since the end of the last glacial maximum at 21 thousand years ago (*28*). A numerical simulation of the GIA process (see supplementary text) based on the V2 model predicts a variation of ~15 m of the current topography along the Orangeburg Scarp, sensu stricto, and an additional ~20 m along the Chippenham and Thornburg Scarps farther north (Fig. 1C). The total along-strike variation is ~35 m. However, uncertainty in the Laurentide ice history and, in particular, the radial profile of mantle viscosity can lead to changes (~10 to 25 m) in the predicted amplitude of the GIA signal (*27*) (fig. S6).

We retrodicted the paleogeography of the East Coast of the United States at maximum flooding by subtracting contributions from GIA and dynamic topography change since 3 Ma from the present topography (Fig. 3). On a regional scale, there is good correspondence between geological data that constrain the known distribution of marine mid-Pliocene sediments, inferred shoreline positions based on the geology (*27*, *36*), and the position of the retrodicted shoreline relative to present sea level. This correspondence suggests that dynamic topography and GIA can account for the vast majority of the warping of the Orangeburg and correlative scarps and the low-relief flooding surface.

Models that retrodict only dynamic subsidence of the U.S. East Coast (*11*, *13*, *14*) over this time interval are not compatible with the observed geology. Furthermore, these models (*13*, *14*) track mantle flow over long time scales (>50 My) starting from the present, and thus any misfit with more

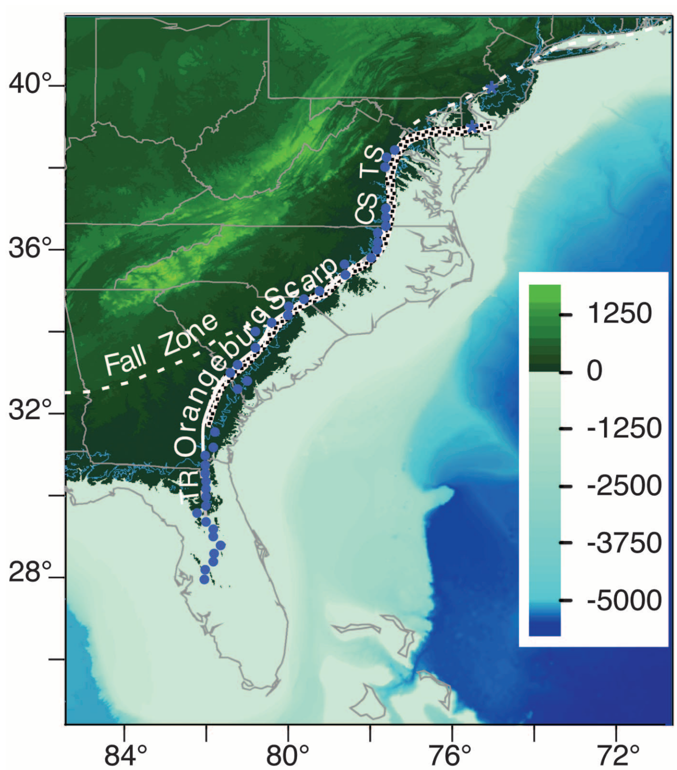

Fig. 3. Retrodicted paleogeography of the Coastal Plain at 3 Ma. Paleogeographic reconstruction of the eastern United States at 3 Ma. Retrodicted topography from which differential dynamic topography based on TX 2007 V2 results and a GIA signal have been subtracted. Scale bar is in meters. No attempt has been made to remove effects of subsequent river and stream incision. Thick dotted line is the shoreline inferred geologically (*23*, *29*) that essentially follows the Orangeburg and correlative scarps. The thin blue line is the +25 m contour on the retrodicted topography. Blue dots are locations for which there are independent outcrop or borehole constraints on the presence of Pliocene marine sediments. Blue stars in southern Delaware and New Jersey are locations of Pliocene estuarine sediments (*38*, *42*).

Downloaded from http://science.sciencemag.org/ on January 24, 2017

recent times (<5 My) implies that these models are unlikely to accurately retrodict dynamic topography at any older time. Our analyses do not support large amplitudes of dynamic topographic subsidence along the Atlantic shelf margin of North America, either on time scales considered here or on longer time scales (30 My) (*10*).

Our simulations have implications for inferences of long-term sea-level change. As can be seen from the retrodicted paleogeography, the Orangeburg and correlative scarps and marine mid-Pliocene localities lie close to the +25 m (Fig. 3 and fig. S4). It would be premature to conclude that this supports an estimate of +25 m for mid-Pliocene sea level because of inherent uncertainties in the various modeling parameters, particularly the mantle viscosity adopted in the dynamic topography and GIA retrodictions, and because we have not included a topographic correction for sediment loading and erosional unloading (supplementary text). Given these uncertainties, our view is that we cannot, as yet, place robust limits on the maximum height of mid-Pliocene sea level.

In the area of the Norfolk Arch, where the largest amplitude of retrodicted dynamic topography change is centered (Fig. 2), the predicted rate of uplift is ~60 m/My (supplementary text). This value is about three times the inferred maximum rate of change of long-term global sea level since the base of the Jurassic (*37*). Moreover, it is greater than ~85% of the rate of change of the short-term global sea-level height when this is averaged over 0.1-My intervals (*37*). Thus, the regression from the Albemarle and southern Salisbury Embayments since mid-Pliocene, which from the local sequence stratigraphic perspective would be directly linked to a significant global sea-level fall, is instead dominated by dynamic topographic uplift and GIA (Fig. 3).

The mid-Pliocene stratigraphy of New Jersey is dominated by regressive sequences, marked by denudation and incision of earlier Miocene flooding surfaces and by deposition of the Pensauken fluvial clastics (*38*). Accepting that New Jersey was rising out of the water (Fig. 3), while Virginia and points south were transgressed, then some other processes, including, but perhaps not limited to, dynamic topography were controlling the sequence stratigraphy of this margin. Because the average slope of the shelf surface is about 0.05° ± 0.025°, even relatively small changes (~20 to 40 m) in dynamic topography beneath the shelf would move the shoreline laterally by tens of km. The regression of the Pliocene and younger sequences from the Albemarle Embayment appears to specifically reflect such an effect, thereby calling into question inferences of sea-level change based on sequence stratigraphic approaches.

Coastal scarps, similar to the Orangeburg scarp but at lower elevations, have often been interpreted as reflecting progressive drops in sea level (*39*, *40*). Alternatively, they may reflect the gradual emergence of the coast under relatively constant sea level at interglacial highstands (*41*). Likely both processes were operating, but it is difficult to disentangle the effects of each over time without also quantifying the mantle dynamic contributions.

Our retrodicted paleogeography at 3 Ma (Fig. 3) closely matches the well-known distribution of mid-Pliocene marine strata in the Albemarle and southern Salisbury Embayments. We suggest that assessments of the height of mid-Pliocene global sea level, and thus the size and stability of the East Antarctic Ice Sheet during this period of relative warmth, must be based on global analyses that account for globally consistent, mantle convection-driven topography, rather than on local investigations.

Note added in proof: Figures 1 and 3 were revised so that the figures in the main text are based on the same dynamic topography and glacial isostatic adjustment calculations.

References and Notes

1. C. L. Drake, M. Ewing, G. H. Sutton, in *Physics and Chemistry of the Earth* (Pergamon, Elmsford, NY, 1959), vol. 3, pp. 110–198.
2. D. McKenzie, *Earth Planet. Sci. Lett.* **40**, 25 (1978).
3. J. V. Browning *et al.*, *Basin Res.* **20**, 227 (2008).
4. M. A. Kominz *et al.*, *Basin Res.* **20**, 211 (2008).
5. A. B. Watts, M. S. Steckler, in *Deep Drilling Results in the Atlantic Ocean; Continental Margins and Paleoenvironment*, M. Talwani, W. Hay, W. B. F. Ryan, Eds. (American Geophysical Union, Washington, DC, 1979), vol. 3, pp. 218–234.
6. A. B. Watts, J. Thorne, *Mar. Pet. Geol.* **1**, 319 (1984).
7. F. Pazzaglia, T. Gardner, *J. Geophys. Res.* **99**, 12143 (1994).
8. H. J. Dowsett, T. Cronin, *Geology* **18**, 435 (1990).
9. K. G. Miller *et al.*, *Science* **310**, 1293 (2005).
10. R. Moucha *et al.*, *Earth Planet. Sci. Lett.* **271**, 101 (2008).
11. C. P. Conrad, C. Lithgow-Bertelloni, K. E. Louden, *Geology* **32**, 177 (2004).
12. R. Moucha, A. M. Forte, S. Quéré, J. X. Mitrovica, D. B. Rowley, *EOS Trans. Am. Geophys. Union* **87**, T53D (2006).
13. R. D. Müller, M. Sdrolias, C. Gaina, B. Steinberger, C. Heine, *Science* **319**, 1357 (2008).
14. S. Spasojević, L. Liu, M. Gurnis, R. D. Müller, *Geophys. Res. Lett.* **35**, 6 (2008).
15. A. M. Forte, J. X. Mitrovica, R. Moucha, N. A. Simmons, S. P. Grand, *Geophys. Res. Lett.* **34**, 5 (2007).
16. W. Dillon, P. Popenoe, "The Blake Plateau Basin and Carolina Trough," in *The Atlantic Continental Margin; U.S.*, R. Sheridan, J. Grow, Eds., of *The Geology of North America* (Geological Society of America, Boulder, CO, 1988), vols. I-2, pp. 291–328.
17. K. O. Emery, E. Uchupi, *The Geology of the Atlantic Ocean* (Springer-Verlag, New York, 1984).
18. C. Poag, W. Sevon, *Geomorphology* **2**, 119 (1989).
19. L. J. Poppe, P. Popenoe, C. W. Poag, B. A. Swift, *Mar. Pet. Geol.* **12**, 677 (1995).
20. N. H. Sleep, *Geophys. J. Int.* **24**, 325 (1971).
21. K. G. Miller, "Sea level change, last 250 million years," in *Encyclopedia of Paleoclimatology and Ancient Environments*, V. Gornitz, Ed. (Springer, Berlin, 2008), pp. 879–893.
22. D. A. Soller, *Geologic and Tectonic History of the Lower Cape Fear Valley, Southeastern North Carolina* (U.S. Geological Survey Professional Paper 1466-A, Government Printing Office, Washington, DC, 1988).
23. H. Dowsett *et al.*, *Stratigraphy* **7**, 123 (2010).
24. D. Fox, *Science* **328**, 1630 (2010).
25. D. J. Hill, A. M. Haywood, R. C. A. Hindmarsh, P. J. Valdes, "Characterizing ice sheets during the Pliocene: Evidence from data and models," in *Deep-Time Perspectives on Climate Change: Marrying the Signal from Computer Models and Biological Proxies*, M. Williams, A. M. Haywood, F. J. Gregory, D. N. Schmidt, Eds. (Geological Society Publishing House, Bath, UK, 2007), pp. 517–538.
26. C. Winker, J. Howard, *Geology* **5**, 123 (1977).
27. D. Krantz, *Quat. Sci. Rev.* **10**, 163 (1991).
28. M. E. Raymo, J. X. Mitrovica, M. J. O'Leary, R. M. Deconto, P. J. Hearty, *Nat. Geosci.* **4**, 328 (2011).
29. P. Adams, N. Opdyke, J. Jaeger, *Geology* **38**, 531 (2010).
30. F. J. Pazzaglia, T. W. Gardner, in *Geomorphology and Global Tectonics*, M. A. Summerfield, Ed. (Wiley Interscience, Chichester, UK, 2000), pp. 284–302.
31. A. M. Forte *et al.*, *Earth Planet. Sci. Lett.* **295**, 329 (2010).
32. R. Moucha *et al.*, *Geophys. Res. Lett.* **36**, L19310 (2009).
33. N. A. Simmons, A. M. Forte, S. P. Grand, *Geophys. Res. Lett.* **34**, 5 (2007).
34. N. A. Simmons, A. M. Forte, S. P. Grand, *Geophys. J. Int.* **177**, 1284 (2009).
35. A. M. Forte, in *Treatise on Geophysics*, G. Schubert, Ed. (Elsevier, Amsterdam, 2007), pp. 805–858.
36. L. W. Ward, R. H. Bailey, J. G. Carter, in *The Geology of the Carolinas: Carolina Geological Society 50th Anniversary Volume*, J. W. Horton Jr., V. A. Zullo, Eds. (Univ. of Tennessee Press, Knoxville, TN, 1991), pp. 274–289.
37. B. Haq, A. Al-Qahtani, *Geoarabia* **10**, 127 (2005).
38. S. D. Stanford, G. M. Ashley, G. J. Brenner, *J. Geol.* **109**, 265 (2001).
39. R. Oaks, N. Coch, J. Sanders, R. Flint, in *Post-Miocene Stratigraphy, Central and Southern Atlantic Coastal Plain*, R. Q. Oaks Jr., J. R. DuBar, Eds. (Utah State Univ. Press, Logan, Utah, 1974), pp. 53–87.
40. R. Oaks, J. DuBar, *Post-Miocene Stratigraphy, Central and Southern Atlantic Coastal Plain* (Utah State Univ. Press, Logan, Utah, 1974), pp. 232–245.
41. M. E. Raymo, L. E. Lisiecki, K. H. Nisancioglu, *Science* **313**, 492 (2006); 10.1126/science.1123296.
42. J. J. Groot, R. R. Jordan, *The Pliocene and Quaternary Deposits of Delaware: Palynology, Ages, and Paleoenvironments*, D. G. Survey, Ed. (Delaware Geological Survey Report of Investigations, Newark, DE, 1999), vol. 58.

Acknowledgments: D.B.R., A.M.F., and J.X.M. thank the Canadian Institute for Advanced Research (CIFAR) for research support and a postdoctoral fellowship to R.M. and members of the Earth Systems Evolution Program of CIFAR for discussions and encouragement. We also acknowledge funding from Natural Sciences and Engineering Research Council of Canada and the Canada Research Chair Program (A.M.F.), the U.S. Department of Energy under contract DE-AC52-07NA27344 (N.A.S.), NSF grants EAR0309189 (S.P.G.) and OCE-1202632 (J.X.M.), and Harvard University (J.X.M.). Work by N.A.S. is performed under the auspices of the U.S. Department of Energy by Lawrence Livermore National Laboratory under contract DE-AC52-07NA27344. Data are available online in the supplementary materials. D.B.R. was responsible for the geology and data integration and thanks T. Komacek for help compiling Pliocene marine localities along the Coastal Plain; A.M.F. and R.M. were responsible for the dynamic topography calculations; J.X.M. for glacial isostatic adjustment calculations; and N.A.S. and S.P.G., for the global seismic tomography, which, working together with A.M.F., yielded the buoyancy field that underlies the dynamic topography calculations.

Supplementary Materials

www.sciencemag.org/cgi/content/full/science.1229180/DC1
Materials and Methods
Supplementary Text
Figs. S1 to S6
Table S1
References (*43–49*)

22 August 2012; accepted 30 April 2013
Published online 16 May 2013;
10.1126/science.1229180

Downloaded from http://science.sciencemag.org/ on January 24, 2017

EXTENDED PDF FORMAT
SPONSORED BY
Sample-Size Antibodies
Now Available
Learn More
R&D SYSTEMS a biotechne brand
www.rndsystems.com

Science AAAS

Dynamic Topography Change of the Eastern United States Since 3 Million Years Ago

David B. Rowley, Alessandro M. Forte, Robert Moucha, Jerry X. Mitrovica, Nathan A. Simmons and Stephen P. Grand (May 16, 2013)

Science **340** (6140), 1560-1563. [doi: 10.1126/science.1229180]
originally published online May 16, 2013

Editor's Summary

By the Sea Side

The Atlantic coastal plain of North America has been thought of as a passive margin, responding mostly to the weight of deposited sediments. As a result, the fine-scale stratigraphy of the sediments has been used to infer changes in global sea level through the Cenozoic. However, recent work has shown that the coastal plain has deformed in response to flow in Earth's mantle. **Rowley *et al.*** (p. 1560, published online 16 May) used a model of flow in the mantle to show that the topography of the mid-Atlantic and Southern United States coast varied by 60 meters or more during the past 5 million years.

This copy is for your personal, non-commercial use only.

Article Tools Visit the online version of this article to access the personalization and article tools:
http://science.sciencemag.org/content/340/6140/1560

Permissions Obtain information about reproducing this article:
http://www.sciencemag.org/about/permissions.dtl

Science (print ISSN 0036-8075; online ISSN 1095-9203) is published weekly, except the last week in December, by the American Association for the Advancement of Science, 1200 New York Avenue NW, Washington, DC 20005. Copyright 2016 by the American Association for the Advancement of Science; all rights reserved. The title *Science* is a registered trademark of AAAS.

Downloaded from http://science.sciencemag.org/ on January 24, 2017